= 378.2 ± 2.4 kcal mol^{-1}.[42] From this approach, $D°(c\text{-}C_5H_4\text{-}H)$ = 105.0 ± 3.4 kcal mol^{-1}, which is the same value as that calculated for the carbanion, $D°(c\text{-}C_5H_4^-\text{-}H)$ = 104.2 ± 7 kcal mol^{-1}.[48] Thus, the presence of five or six π-electrons does not influence the C-H bond strengths in these two molecules.

Conclusions

A flowing afterglow coupled with a CW laser system has been developed for the accurate determination of electron affinities of neutral molecules from threshold measurements of EPD of the corresponding negative ions. With this apparatus, the EPD thresholds of the doublet ground state of cyclopentadienylidene anion radical, $c\text{-}C_5H_4^{\bullet-}$, yielding the ground ($^3B_1$ at 708 nm) and certain excited states ($^1A_2$ at 619 nm, $^3A_2$ at 598 nm, and, tentatively, $^1A'$ at 576 nm) of the corresponding carbene have been measured. From these data and the previously determined $\Delta H°_{f,298}(c\text{-}C_5H_4^{\bullet-})$, the $\Delta H°_{f,298}(c\text{-}C_5H_4)$ for the ground and excited states are calculated. It is further shown that the C-H bond dissociation energies in $c\text{-}C_5H_5^{\bullet}$ and $c\text{-}C_5H_5^-$ are the same within the broad error limits.

Acknowledgment. We thank the National Science Foundation for support of this research and Professor D. W. Setser for a number of suggestions and helpful discussions. We also thank Mr. John Linzi for design and construction of the circuit that allowed for recovery of the eight digits of data from the photon counter/processor.

Registry No. $C_6H_5C(=O)CH_2^{\bullet}$, 50781-28-7; $c\text{-}C_5H_5^-$, 12127-83-2; $c\text{-}C_5H_5^{\bullet}$, 2143-53-5; $c\text{-}C_5H_4^{\bullet-}$, 75137-28-9; $c\text{-}C_5H_4$, 4729-01-5; acetophenone enolate anion, 34438-71-6.

(48) $\Delta H°_{f,298}(c\text{-}C_5H_5^-)$ = 19.6 ± 3.8 kcal mol^{-1}.[43]

Electronic Excitation in Low-Energy Collisions: A Study of the Collision-Induced Dissociation of Nitromethane Ion by Crossed-Beam Tandem Mass Spectrometry

Kuangnan Qian, Anil Shukla, and Jean Futrell*

Contribution from the Department of Chemistry and Biochemistry, University of Delaware, Newark, Delaware 19716. *Received December 14, 1990*

Abstract: The dynamics of collision-induced dissociation (CID) of nitromethane ion have been investigated with an angle-resolved crossed-beam tandem mass spectrometer. Kinetic energy and angular distributions of two main products of the dissociation, NO^+ and NO_2^+, were measured at center-of-mass (CM) collision energies from 1.5 to 119 eV. Impulsive mechanisms are involved for NO_2^+ formation at all energies investigated. At and below 3-eV collision energy, a rebound reaction mechanism is observed, implying small impact parameter collisions dominate the CID process. A transition from backward to forward scattering is observed for NO_2^+ in the collision energy range of 3–6 eV. At higher energies, NO_2^+ formation is progressively more forward scattered but never approaches zero scattering angle within the energy range studied. The mechanism for forming NO^+ is uniquely different from NO_2^+ in that two intensity maxima are observed at all energies, suggesting that the dissociation proceeds via at least two reaction pathways. The peak maximum at 0° is attributed to dissociation following isomerization of nitromethane ion to methyl nitrite ion while the back-scattered peak follows an impulsive excitation reaction path similar to NO_2^+ formation and is attributed to nonisomerized nitromethane cations that require small impact parameter collisions to induce isomerization and dissociation. As the collision energy is increased, a highly endothermic dissociation process involving the transfer of 5.5–5.7-eV energy from translational to internal energy is also observed. Since the threshold for NO^+ formation is only 0.64 eV, it is suggested that these low-energy collisions lead to electronic excitation of nitromethane ion to the sixth ionization band of its photoelectron spectrum and that dissociation proceeds on the excited-state hypersurface.

Introduction

The unimolecular and collision-induced dissociation (CID) of the nitromethane ion and its isomer, methyl nitrite ion, have been extensively studied.[1-13] It has often been suggested[2,3,7] that their dissociation involves isolated electronic states and incomplete internal energy randomization in violation of the fundamental assumption of statistical theories—e.g., the Rice-Ramsperger-Kassel-Marcus (RRKM) theory of unimolecular reactions[14] and the quasi-equilibrium theory (QET) of mass spectra.[15] The present CID dynamics study was undertaken, in part, to search for reactive scattering features that might support this hypothesis. A preliminary account reporting such dynamics features has already been published.[16]

We have shown in previous publications that photoelectron spectra and experimentally determined breakdown graphs provide information useful for the interpretation of CID scattering experiments.[17] The photoelectron spectrum of nitromethane and its ionic breakdown graph measured by photoelectron-photoion coincidence (PEPICO) technique are shown in Figure 1. The thermochemically predicted onsets and experimentally measured dissociation energies for different dissociation processes are listed in Table I. The breakdown graph for the nitromethane ion shows[2] that the formation of NO^+ proceeds via at least two different

(1) Lifshitz, C.; Rejwan, M.; Levin, I.; Peres, T. *Int. J. Mass Spectrom. Ion Processes* **1988**, *84*, 271.
(2) Niwa, Y.; Tajima, S.; Tsuchinya, T. *Int. J. Mass Spectrom. Ion Phys.* **1981**, *40*, 287.
(3) Ogden, I. K.; Shaw, N.; Danby, C. J.; Powis, I. *Int. J. Mass Spectrom. Ion Phys.* **1983**, *54*, 41.
(4) Egsgaard, H.; Carlsen, L.; Elbel, S. *Ber. Bunsen-Ges. Phys. Chem.* **1986**, *90*, 369.
(5) Baer, T.; Hass, J. R. *J. Phys. Chem.* **1986**, *90*, 451.
(6) Ferguson, E. E. *Chem. Phys. Lett.* **1987**, *138*, 450.
(7) Gilman, J. P.; Hsieh, T.; Meisels, G. G. *J. Chem. Phys.* **1983**, *78*, 1174.
(8) (a) Meisels, G. G.; Hsieh, T.; Gilman, J. P. *J. Chem. Phys.* **1980**, *73*, 4126. (b) Gilman, J. P.; Hsieh, T.; Meisels, G. G. *J. Chem. Phys.* **1983**, *78*, 3767.
(9) Sirois, M.; Holmes, J. L.; Hop, C. E. C. A. *Org. Mass Spectrom.* **1990**, *25*, 167.
(10) Todd, P. J.; Warmack, R. J.; McBay, E. H. *Int. J. Mass Spectrom. Ion Phys.* **1983**, *50*, 299.
(11) Zwinselman, J. H.; Nacson, S.; Harrison, A. G. *Int. J. Mass Spectrom. Ion Processes* **1985**, *67*, 93.
(12) Hubick, A. R.; Hemberger, P. H.; Laramee, J. A.; Cooks, R. G. *J. Am. Chem. Soc.* **1980**, *102*, 3997.
(13) McKee, M. L. *J. Phys. Chem.* **1986**, *90*, 2335.
(14) Marcus, R. A.; Rice, O. K. *J. Phys. Colloid Chem.* **1951**, *55*, 894.
(15) Rosenstock, H. M.; Wallenstein, M. B.; Wahrhaftig, A. L.; Eyring, H. *Proc. Natl. Acad. Sci. U.S.A.* **1952**, *38*, 667.
(16) Qian, K.; Shukla, A.; Futrell, J. *Rapid Commun. Mass Spectrom.* **1990**, *4*, 222.
(17) Qian, K.; Shukla, A.; Futrell, J. *J. Chem. Phys.* **1990**, *92*, 5988.

0002-7863/91/1513-7121$02.50/0

Table I

Ionization Energies of Nitromethane

band	vertical IP (eV)[a]	vertical IP (eV)[b]	adiabatic IP (eV)[b]	band	vertical IP (eV)[a]	vertical IP (eV)[b]	adiabatic IP (eV)[b]
1	11.28	11.32	11.07	5	15.83	15.75	–
2	11.69	11.73	11.73	6	17.42	17.45	−16.7
3	11.69	–	–	7	17.42	–	
4	14.72	14.73	13.85	8	18.9	19.1	

Fragment Ion Appearance Energies from Nitromethane

	ionization or appearance energy (eV)					
ionization process	Lifshitz et al.[c]	Ogden et al.[d]	Niwa et al.[e]	Gilman et al.[f]	Kandel[g]	thermochemical onset[h]
$CH_3NO_2 \rightarrow CH_3NO_2^{\bullet+} + e$	11.1			11.12		11.02
$\rightarrow NO^+ + CH_3O^{\bullet}(CH_2OH)$	11.75	11.5	11.7	11.76	12.01	11.15 (10.72)
$\rightarrow NO_2^+ + CH_3^{\bullet}$	12.1	11.97	12.1	12.34	12.47	12.34
$\rightarrow CH_3^{\bullet+} + NO_2$			−13.6		13.58	12.46

[a] Taken from ref 18. [b] Taken from ref 38. [c] Reference 1. [d] Reference 3. [e] Reference 2. [f] Reference 7. [g] Reference 45. [h] Calculated for ground-state reactants and products by using data from ref 46.

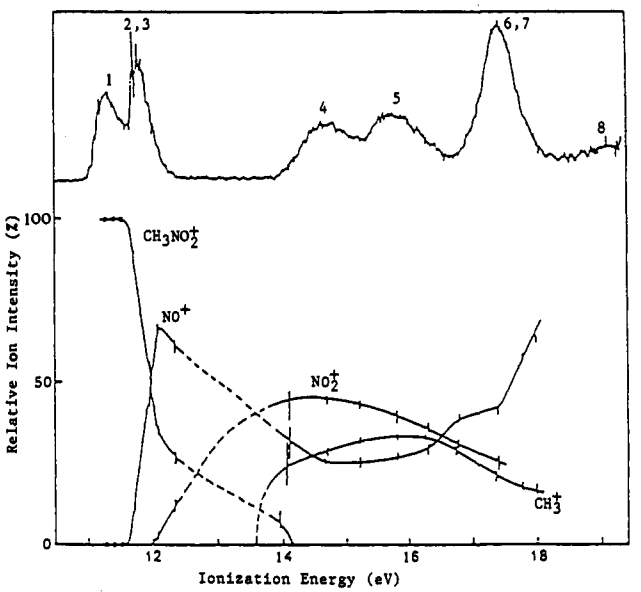

Figure 1. He(I) photoelectron spectrum and breakdown diagram of nitromethane. The numbers marked on the spectrum correspond to electronic states following ref 18. Reprinted from ref 2 with kind permission of Elsevier Scientific Publishing Co.

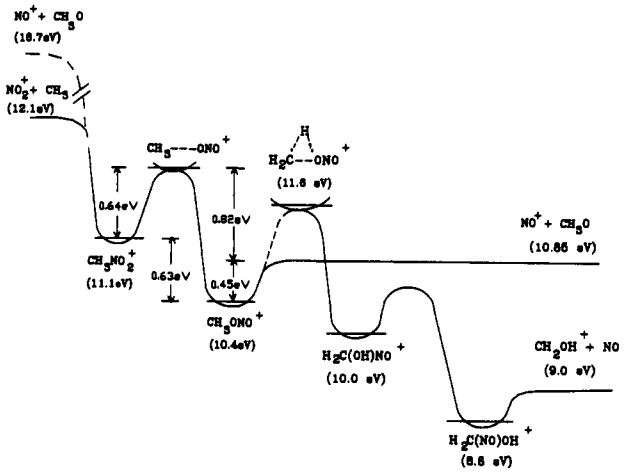

Figure 2. Schematic potential energy diagram for the dissociation of nitromethane ion to NO_2^+ and NO^+, adapted from ref 7 with additional data on dissociation characteristics of the methyl nitrite cation (T. Baer, private communication).

mechanisms. At low energy, the appearance energy of NO^+ is 0.8 eV higher than the thermochemical onset and involves a potential energy barrier to isomerization to an excited methyl nitrite structure. The second mechanism is manifested as a sharp rise of the NO^+ breakdown curve at an internal energy 5.7 eV above the ground state (and in coincidence with the energy of the sixth electronic state of nitromethane ion[18]) as shown in Figure 1. This second mechanism for NO^+ formation was pointed out by Niwa et al.[2] but not discussed in any detail by these researchers. Ogden et al.[3] suggested that NO^+ could be produced at this energy from the secondary dissociation of NO_2^+.

Gilman et al.[7,8] and Ogden et al.[3] rationalized the low-energy mechanism by proposing that the nitromethane ion isomerizes to the methyl nitrite ion structure prior to dissociating into NO^+. The higher appearance energy was attributed to the energy barrier for isomerization. These suggestions are included in Figure 2, a schematic illustration of the potential energy hypersurface that is based, in part, on the PEPICO measurements and interpretation of Gilman et al.[7] The transition states and their energetics in the decomposition of the methyl nitrite cation are based, in part, on unpublished work of Baer et al.[19] The direct bond cleavage into $NO^+ + CH_3O^{\bullet}$ occurs on a single diabatic surface, while the production of CH_3O^+ occurs in a long-range curve crossing to a different diabatic surface, as pointed out by Leyh-Nihant and Lorquet.[20] Deformed CH_3O^+ ions formed via this mechanism immediately rearrange to the CH_2OH^+ structure.

For the complementary dissociation of $CH_3NO_2^{\bullet+}$ to $NO_2^+ + CH_3^{\bullet}$ and $CH_3^{\bullet+} + NO_2$, the appearance energy of $CH_3^{\bullet+}$ is significantly higher than that of NO_2^+ although they have nearly the same thermochemical onsets. This was taken as evidence that the two reactions proceed from different electronic hypersurfaces. The $^2A_1$ ground state and $^2B_2$ and $^2A_2$ excited states of $CH_3NO_2^{\bullet+}$ are overlapping levels in the photoelectron spectrum of CH_3NO_2 shown in Figure 1. The dissociation to form $NO_2^+(^1A_1)$ and $CH_3(^2A_2'')$ correlates with the $^2A_1$ ground state of $CH_3NO_2^{\bullet+}$, while the overlapping second and third bands interconvert to this level. The alternative $CH_3^+(^1A_1')$ and $NO_2(^2A_1)$ products correlate with a highly excited $^2A_1$ state, which is observed at ~16.7 ev in the photoelectron spectrum.[2] Since the onset for the observation of $CH_3^{\bullet+}$ is ~13.6 eV, this dissociation path correlates with higher excited states $^2B_2$ or $^2B_1$ corresponding to the dissociation limits of 13.57 and 14.05 eV, respectively. The latter correlates with $^2B_1$ or $CH_3NO_2^{\bullet+}$, the third ionization band. It is therefore quite clear that the two dissociations proceed from different electronic states.

Cooks and co-workers[12] have studied the two principal CID products, NO^+ and NO_2^+, using angle-resolved mass spectrometry

(18) Kimura, K.; Katsumata, S.; Achiba, Y.; Yamazaki, T.; Iwata, S. *Handbook of Hel Photoelectron Spectra of Fundamental Organic Molecules*; Halsted Press: New York, 1981.

(19) Baer, T.; Morrow, J. C.; Dutuit, O. To be published.

(20) Leyh-Nihant, B.; Lorquet, J. C. *J. Chem. Phys.* **1988**, *88*, 5606.

(ARMS). Although the reaction producing NO^+ has a lower onset energy than NO_2^+, the ratio of NO^+/NO_2^+ actually increases with scattering angle. This is an unexpected result since internal energy deposition generally increases with scattering angle. This anomalous ARMS result can be interpreted as evidence for participation of the high-energy mechanism for NO^+ formation shown in Figure 1. Alternatively, since Todd et al.[10] have shown that broad angular distributions accompanying kinetic energy release on dissociation account for much of the scattering observed in ARMS, the isomerization barrier for NO^+ formation (which provides a mechanism for depositing excess translational energy into the NO^+ product ion) can also account for the ARMS results. Our beam experiments, which measure both energy exchange and angular scattering, clearly distinguish between these two hypotheses.

Harrison and co-workers[11] observed results complementary to those of Cooks et al.[12] using a triple quadrupole mass spectrometer. Since quadrupole mass filters have larger acceptance angles than sector instruments, they exhibit correspondingly higher collection efficiency for fragment ions scattered at large angles. Since they also observed an increasing NO^+/NO_2^+ ratio with increasing ion collision energy, they tentatively excluded kinetic energy release on dissociation as the major factor. By comparing their data with PEPICO results and noting that the nitromethane ion preferentially dissociates into NO^+ above 5.5-eV internal energy, they concluded that the collision process excites the molecular ion in the 5–7-eV internal energy range. In the breakdown curve of Figure 1, this corresponds to the second rise of NO^+ relative abundance.

Harrison et al.[11] also investigated change exchange of nitromethane with various ions of known recombination energies (CS_2^+, 10.2 eV; COS^+, 11.2 eV; Xe^+, 12.5 eV; N_2O^+, 12.9 eV; CO^+, 14.0 eV; N_2^+, 15.6 eV; and Ar^+, 15.8 eV). These experiments produced relative amounts of NO^+ and NO_2^+ in qualitative agreement with PEPICO results in the lower internal energy range. Specifically, the ratio NO_2^+/NO^+ increased monotonically with ion internal energy. From the comparison of these results with CID, they concluded that energy transferred by ion–neutral collision is *much larger* for nitromethane ions than is usually observed in low and moderate collision energy CID.

The question whether nonstatistical dissociations are important mechanisms for nitromethane and methyl nitrite cations has been critically examined by Baer and Haas[5] and by Lifshitz et al.[1] Baer and Haas have shown that the competition between rearrangement to a lower energy isomer, which they represent as $HNC(OH)_2^{\bullet+}$, and the resulting double minimum potential in which $H_2COH^{\bullet+}(+NO)$ and $NO^+(+CH_3^{\bullet})$ are formed in two different reaction pathways explains many of the anomalies reported for the methyl nitrite cation. Consideration of nitromethane cation rearrangement to methyl nitrite cation suggests that at least three minima and four transition states are important features of the potential surface. Ab initio studies of isomer geometries by these researchers provided the necessary information to calculate QET/RRKM rates that satisfactorily rationalized most of the PEPICO and kinetic energy release distributions (KERD's)[10] for methyl nitrite. This problem has been further investigated by using dispersed synchrotron radiation to obtain more precise data and higher level calculations to characterize hypersurface potential minima and transition states.[19]

Lifshitz et al.[1] recently reported a thorough study of the unimolecular fragmentation of the nitromethane cation by photoionization and tandem mass spectrometry. In combination with accurate information on neutral and ionic heats of formations, structural information from the CID studies, and accurate appearance energy measurements, these workers demonstrated that the four principal unimolecular dissociation reactions

$$CH_3NO_2^{\bullet+} \rightarrow CH_2NO^+ + OH^{\bullet} \quad (1)$$

$$CH_3NO_2^{\bullet+} \rightarrow NO^+ + CH_3O^{\bullet} \quad (2)$$

$$CH_3NO_2^{\bullet+} \rightarrow NO_2^+ + CH_3^{\bullet} \quad (3)$$

$$CH_3NO_2^{\bullet+} \rightarrow CH_2NO_2^+ + H^{\bullet} \quad (4)$$

are all in competition at threshold and that reaction 1 exhibits no kinetic shift. Most (but not all) of the anomalies discussed by previous researchers as examples of nonergodic behavior were resolved satisfactorily by this study. It was demonstrated that a number of "hidden" hydrogen transfers are important features of the critical path(s) between reactant and product ions. Important rearrangement structures include the aci form of nitromethane cation (which is the precursor for reactions 1 and 4, not studied in this research) and the methyl nitrite cation. Further, it was strongly inferred that ion–dipole complexes were important intermediates in the decomposition of both methyl nitrite and nitromethane cations. The inclusion of these intermediate species in the mechanisms for the four reactions investigated made it possible to rationalize their observations satisfactorily within the QET/RRKM framework. Several of these features are illustrated schematically in Figure 2, which summarizes salient points from previous studies of the unimolecular dissociation of nitromethane and methyl nitrite ions.

An important finding in this research[1] is that reactions 1, 2, and 4 occur as metastable ions and have the same appearance energy. Evidently a common transition state is accessed for all three reactions, two of which involve isomerization to *aci*-nitromethane (reactions 1 and 4) and one of which involves isomerization to the methyl nitrite cation (reaction 2). It was suggested that this critical transition state was an ion–dipole complex $[CH_3^+ \cdots NO_2]^{\bullet}$ which subsequently rearranges either to *aci*-nitromethane or methyl nitrite cation in a narrow energy range above threshold. The theoretical study by McKee[13] supports this interpretation. At higher energy, the transition is rapid and the system passes diabatically by intramolecular charge transfer to form the NO_2^+ product, reaction 2. This common transition state has a marked influence on the reaction dynamics of the unimolecular dissociation of the nitromethane cation. This explanation accounts for the gradual rise of the photoionization efficiency curve for NO_2^+ generation, reaction 3, and for the sharp rise about 1 eV above threshold, when the isomerization reaction channels no longer compete. We anticipate these features will also influence CID reaction dynamics, and a modified ion–dipole complex is shown as the rearrangement barrier transition state in Figure 2.

As noted, the recent ab initio calculations by McKee[13] identify the major potential energy wells and probable transition states for nitromethane, *aci*-nitromethane, and methyl nitrite cation decomposition pathways. This calculation provides strong support for the participation of charge transfer and ion dipole complexes in addition to the stable cations. Plausible structures are suggested for transition states for the principal decomposition pathways. This paper, in combination with the QET/RRKM calculations of Lifshitz et al.,[1] Lorquet et al.,[19,21] and Baer et al.,[5] provides a comprehensive picture of the lowest energy decomposition channels for both methyl nitrite and nitromethane cations. In particular, they account for the nonobservation of $CH_3O^{\bullet+}$ or NO_2^+ as metastable ions from nitromethane ions while a strong metastable for NO^+ is observed. NO_2^+ is observed only as a CID product, while NO^+ is generated both by CID and as a unimolecular dissociation product, both proceeding via a prior rearrangement to methyl nitrite. We may also infer, from the complex multiminimum, multimaximum potential surface described, that CID reactions may proceed too rapidly for the system to explore all the minima requiring complex rearrangements. (For an informative discussion of probabilities for following diabatic vs adiabatic surfaces in dissociation of methyl nitrite and nitromethane cations and the possible role of ion–dipole complexes, see refs 19 and 21.)

The present research has concentrated on two principal CID reactions of nitromethane ion at center-of-mass (CM) collision energies ranging from 1.5 to 119 eV. This system was selected specifically as a second example for which non-QET/RRKM dissociation has been reported. Two collision gases were used

$$CH_3NO_2^{\bullet+} + Ar\ (He) \rightarrow NO_2^+ + CH_3^{\bullet} + Ar\ (He) \quad (5)$$

$$CH_3NO_2^{\bullet+} + Ar\ (He) \rightarrow NO^+ + CH_3O^{\bullet} + Ar\ (He) \quad (6)$$

(21) Lorquet, J. C.; Barbier, C.; Leyh-Nihant, B. *Adv. Mass Spectrom.* **1986**, *10*, 71.

to check whether there were any features attributable to specific neutral colliders like those reported previously.[16] On the basis of the foregoing discussion, we also anticipated that most of our scattering results, if not all, might be interpretable within the framework of the QET/RRKM mechanism.

Experimental Section

The angle-resolved crossed-beam tandem mass spectrometer used in this study has been described in detail elsewhere,[22] and only a brief outline is given here. A VG-7070E double-focusing mass spectrometer equipped with a standard electron ionization source provides 3-keV nitromethane molecular ions. The ion beam from this spectrometer is decelerated by a series of cylindrical and rectangular tube lenses to the desired energy at the collision center and collided with a vertically moving supersonic beam of helium or argon atoms generated by supersonic expansion through a 100-μm nozzle and collimated by a 1-mm-diameter skimmer. Energy and mass analyses of fragment ions are performed by a hemispherical energy analyzer and a quadrupole mass filter, respectively. The complete detector assembly is rotated about the collision center to obtain energy and intensity distributions as a function of laboratory scattering angle. The typical ion beam used in this work has an energy spread of ~1 eV fwhm and angular spread of ~1° fwhm.

The data obtained directly from the instrument are energy distributions of a specific fragment ion at various angles. These data are transformed into velocity contour diagrams in the CM frame, where the probability of finding the fragment ion is mapped in Cartesian velocity coordinates. The transformations from energy space to velocity space, from polar coordinate to Cartesian coordinate, and from laboratory frame to the CM frame are based upon the Jacobian transformation of variables and have been fully discussed elsewhere.[23,24] The transformation procedure specific to our experimental data has also been described.[25]

The relative translational energy distribution of the fragment ion is derived from the integration over all scattering angles of the CM velocity contour map using the relationship[26]

$$P(T) = u \int P(u_1,u_2,u_3) \sin \chi \qquad (7)$$

where u is the magnitude of the product velocity vector with respect to the CM; $P(u_1,u_2,u_3)$ is the probability that products are observed in the space defined by the Cartesian CM coordinates, u_1, u_2, and u_3, and χ is the CM scattering angle. The most probable energy transfer ΔT is deduced from the difference between final and initial relative translational energy and used to construct ΔT circles in the velocity contour diagrams. These circles represent the loci of velocity vectors for the activated $CH_3NO_2^{*+}$, which recoils from the CM with the same product translational velocity. Since velocity contour diagrams may distort the relative importance of dynamic features they display, analysis of relative CID cross sections requires the construction of energy distributions using eq 7.

Results and Discussion

Before our experimental data is discussed, it should be pointed out that there is a fundamental limitation in beam experiments which explore the reaction dynamics of CID processes—namely, that two particles collide and a minimum of three leave the scattering center. Only the product ion velocity vector is measured, and the scattering angles and velocities of the two neutral species can have all values allowed by conservation of energy and angular momentum. Consequently one cannot construct a scattering diagram that uniquely determines the energetics and angular properties of CID reactions. This dilemma is resolved by the assumption that there is a time delay between the excitation process and the decomposition of the excited ion. We think that this generally accepted assumption is very well founded, especially for polyatomic ions, as the time delay need only be long enough for the neutral collider to escape the potential field of the ion. For typical collisions, this will be much less than 10^{-13} s. Since the decomposition step is preceded by at least one and typically by thousands to millions of vibrational oscillations, we make this key assumption in constructing all the scattering diagrams presented in this paper.

The discussion of CID reaction dynamics is further simplified if we assume there is negligible kinetic energy release in the dissociation of the excited polyatomic ion. With this assumption, the fragment ion scattering pattern properly reflects the scattering properties of its excited parent ion precursor. Kinetic energy release simply broadens the distribution, and the most probable velocity distribution for daughter ions accurately mirrors the most probable distribution of parent ions (assuming random orientations of the dissociating ion). These assumptions have been discussed in some detail[25] elsewhere.

Scattering data are presented in the form of CM Cartesian velocity contour diagrams in Figures 3–8 and 10–13. In these

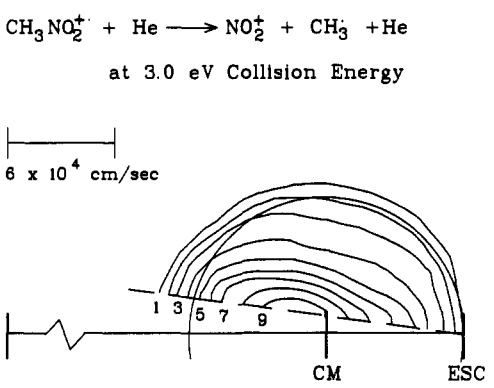

Figure 3. CM velocity contour map for the CID of nitromethane ion to NO_2^+ on collision with He at 3.0-eV collision energy. CM and ESC denote center-of-mass and elastic scattering circle, respectively, and the numbers represent relative intensities of each contour.

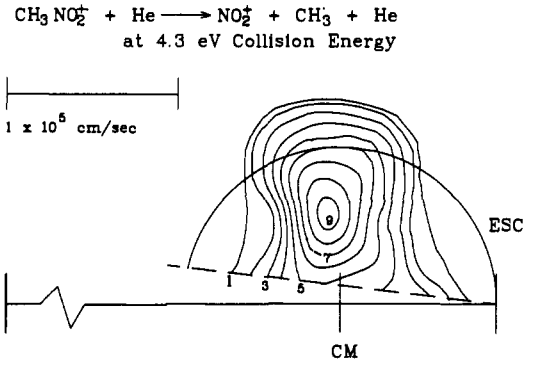

Figure 4. CM velocity contour map for the CID of nitromethane ion to NO_2^+ on collision with He at 4.3-eV collision energy. CM and ESC denote center-of-mass and elastic scattering circle, respectively, and the numbers represent relative intensities of each contour.

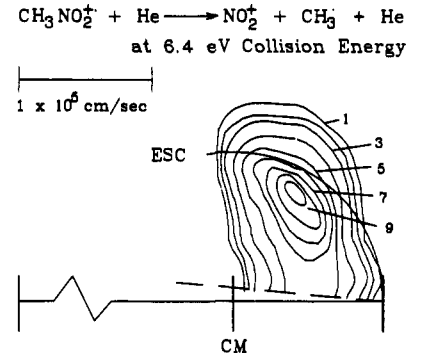

Figure 5. CM velocity contour map for the CID of nitromethane ion to NO_2^+ on collision with He at 6.4-eV collision energy. CM and ESC denote center-of-mass and elastic scattering circle, respectively, and the numbers represent relative intensities of each contour.

(22) Shukla, A. K.; Anderson, S. G.; Howard, S. L.; Sohlberg, K. W.; Futrell, J. H. *Int. J. Mass Spectrom. Ion Processes* **1988**, *86*, 61.
(23) Birkinshaw, K.; Pacak, V.; Herman, Z. In *Interactions Between Ions and Molecules*; Ausloos, P., Ed.; Plenum: New York, 1974.
(24) Friedrich, B.; Herman, Z. *Collect. Czech. Chem. Commun.* **1984**, *49*, 570.
(25) Shukla, A. K.; Qian, K.; Anderson, S.; Futrell, J. H. *J. Am. Soc. Mass Spectrom.* **1990**, *1*, 6.
(26) Wolfgang, R.; Cross, R. J., Jr. *J. Phys. Chem.* **1969**, *73*, 743.

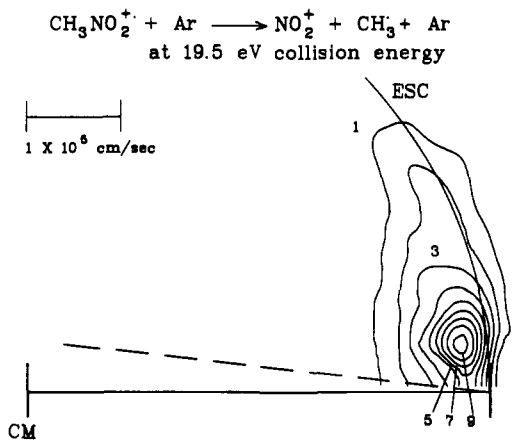

Figure 6. CM velocity contour map for the CID of nitromethane ion to NO_2^+ on collision with Ar at 19.5-eV collision energy. CM and ESC denote center-of-mass and elastic scattering circle, respectively, and the numbers represent relative intensities of each contour.

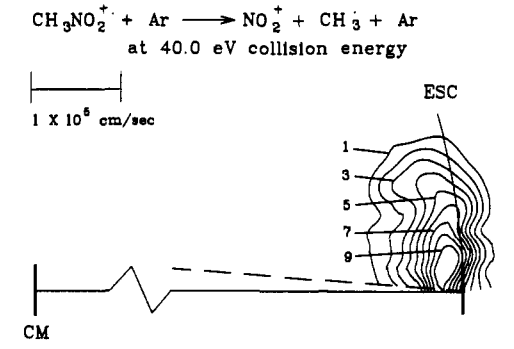

Figure 7. CM velocity contour map for the CID of nitromethane ion to NO_2^+ on collision with Ar at 40.0-eV collision energy. CM and ESC denote center-of-mass and elastic scattering circle, respectively, and the numbers represent relative intensities of each contour.

figures, the CM velocity vectors of product ions are plotted as contours of equal relative intensity ranging from 1 to 9 for NO_2^+ and NO^+ as a function of collision energy. Only positive scattering angles are shown; symmetry about the relative velocity requires identical distributions for negative scattering angles. Each diagram includes the CM velocity designated by a vertical bar and the elastic scattering circle, ESC, as important reference indices. (The dashed line in this figure defines the region in which ions cannot be detected by our instrument because of geometric constraints.[25])

Direct C–N Bond Cleavage. Formation of NO_2^+. Although the threshold energy for reaction 5 is 1 eV, we did not obtain sufficient net counts of NO_2^+ at collision energies below 3 eV to plot a contour map with reasonable accuracy. This indicates that the CID cross section for this dissociation process is small at low collision energies. This behavior is quite different from our results for acetone[27] and propane ion[28] CID and many other systems studied with triple quadrupole spectrometers[29,30] where fragmentation has been observed at or below the thermochemical threshold. Since molecular ions were formed by 70-eV electrons in all these experiments, it is expected that some nitromethane ions would be vibrationally excited, leading to CID fragmentation at and below the thermochemical threshold energies for ground-state ions. However, this was not observed for reaction 5. Below 3 eV, the relative abundance of NO_2^+ is lower than NO^+. As the ion collision energy is increased above 3 eV, the relative

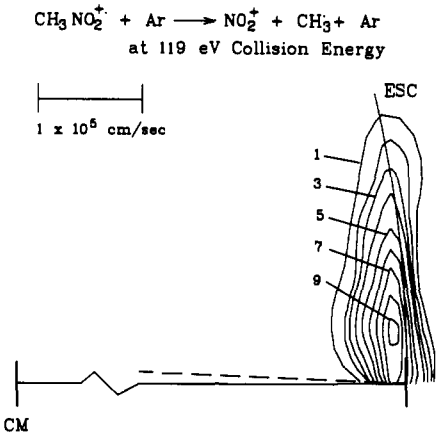

Figure 8. CM velocity contour map for the CID of nitromethane ion to NO_2^+ on collision with Ar at 119.0-eV collision energy. CM and ESC denote center-of-mass and elastic scattering circle, respectively, and the numbers represent relative intensities of each contour.

intensity of NO_2^+ becomes higher than NO^+ and remains so up to 119 eV, the highest collision energy we have studied.

Since formation of NO^+, reaction 6, requires less energy than NO_2^+ formation, it is expected—and observed—that low-energy CID would be dominated by NO^+ rather than NO_2^+ fragment ions at and just above the threshold energy for these reactions. This behavior is in agreement with breakdown curves (Figure 1) for nitromethane ion determined by PEPICO[2] and charge exchange mass spectrometry.[11] We do not observe the second crossing point of NO^+/NO_2^+ relative intensity reported by Cooks et al.,[12] who find the intensity of NO^+ is higher than NO_2^+ above 10-eV collision energy. This contradiction may be related to the fact that our experiments have all been performed under single collision conditions with beam attenuations much less than 5% while all other CID studies have been performed with higher beam attenuations. It is routine in CID studies to attenuate the primary beam by 50%, or even more. For collision probability of 0.5, the probability[31] of two collisions occurring is ~9% and three collisions is ~3%. Multiple collisions would result in more energy transfer and could also cause secondary decompositions to occur—e.g., $NO_2^+ \rightarrow NO^+ + O$—in collision chamber experiments. These secondary processes cannot occur in our crossed-beam experiments.

Figure 3 shows the velocity contour map for reaction 5 at 3-eV CM collision energy. The scattering maximum in this diagram is in the backward-scattered region with a scattering angle greater than 170°. Backward scattering suggests that nitromethane ion and helium neutral collide via very small (perhaps zero) impact parameters. Activated $CH_3NO^{+\cdot *}$ ions rebound from the CM with activation induced primarily by the ion–neutral repulsive part of the potential surface and dissociate into NO_2^+ and corresponding neutral fragments. (Considering small signal intensity and experimental errors in its measurements, it may be argued that this contour diagram is centered at the CM for the $CH_3NO_2^{+\cdot}$/He collision with nearly all the translational energy converted into internal energy. However, the $P(T)$ diagram derived from eq 7 (discussed later) clearly demonstrates otherwise.)

The backward-scattered peak in Figure 3 is similar to that observed in the CID of acetone ions at CM collision energies below 2.4 eV where both superelastic and inelastic CID products are backward scattered.[17] Backward scattering has also been invoked to explain high molecular weight ion CID at kiloelectronvolt laboratory energies.[32] In fact, when kiloelectronvolt laboratory energy is transformed into CM collision energy for high-mass ions colliding with He, collision energy falls within the range reported here. CID processes that proceed via small impact parameter collisions for the activation process will result in backward

(27) Shukla, A. K.; Qian, K.; Howard, S. L.; Anderson, S. G.; Sohlberg, K. W.; Futrell, J. H. *Int. J. Mass Spectrom. Ion Processes* **1989**, *92*, 147.
(28) Shukla, A. K.; Qian, K.; Anderson, S. G.; Futrell, J. H. *Int. J. Mass Spectrom. Ion Processes*, submitted for publication.
(29) Douglas, D. J. *J. Phys. Chem.* **1982**, *86*, 185.
(30) Dawson, P. H.; Sun, W. *Int. J. Mass Spectrom. Ion Processes* **1986**, *70*, 97.
(31) Smith, D. L.; Futrell, J. H. In *Dynamic Mass Spectrometry*; Price, D., Ed.; Heyden: New York, 1978.
(32) Neumann, G. M.; Shell, M. M.; Derrick, P. J. *Z. Naturforsch.* **1984**, *39A*, 584.

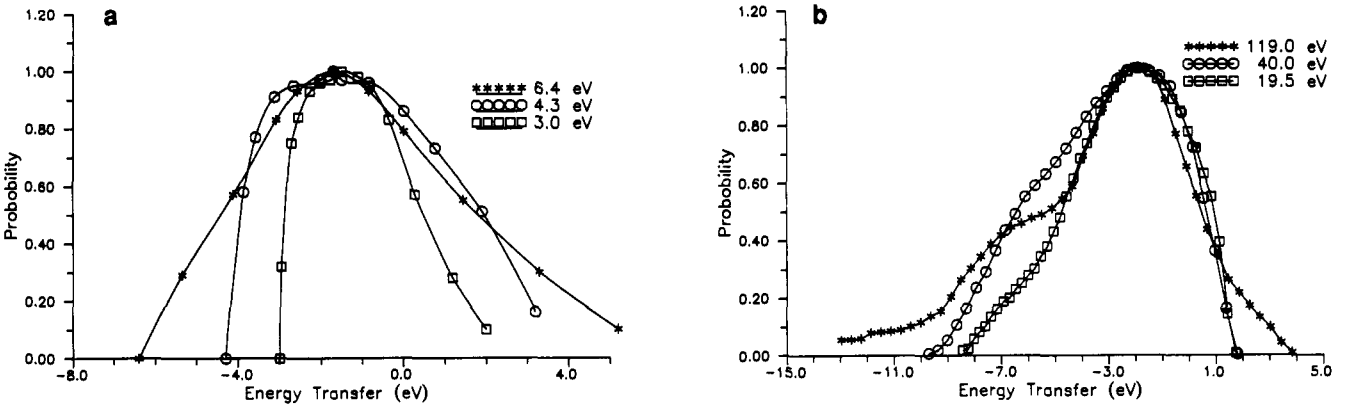

Figure 9. Relative translational energy distribution ($P(T)$) of NO_2^+ ions obtained from Figures 2–7 using eq 7: (a) 3.0-, 4.3-, and 6.4-eV collision energy, (b) 19.5-, 40.0-, and 119.0-eV collision energy.

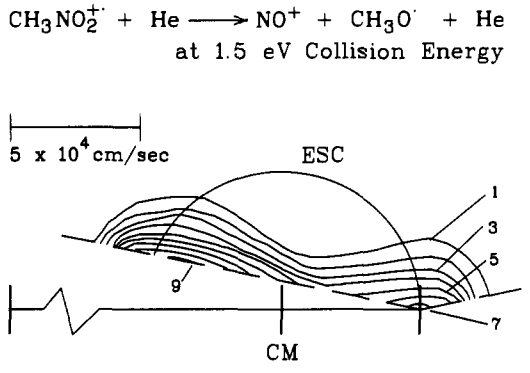

Figure 10. CM velocity contour map for the CID of nitromethane ion to NO^+ on collision with He at 1.5-eV collision energy. CM and ESC denote center-of-mass and elastic scattering circle, respectively, and the numbers represent relative intensities of each contour.

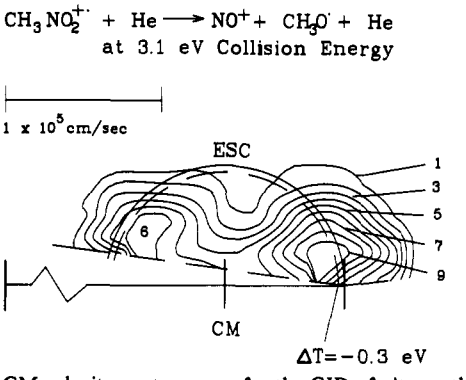

Figure 11. CM velocity contour map for the CID of nitromethane ion to NO^+ on collision with He at 3.1-eV collision energy. CM and ESC denote center-of-mass and elastic scattering circle, respectively, and the numbers represent relative intensities of each contour.

scattering in the CM frame. However, back-scattering is not observed at any energy in the CID of propane ions[25,28,33] (an archetypical example of QET/RRKM behavior) where only forward scattering occurs even at a CM collision energy as low as 1.7 eV.

Figure 4 shows the velocity contour diagram for reaction 5 at the slightly higher collision energy of 4.3 eV. A distinct change from Figure 3 is that the most probable scattering angle has dramatically decreased to about 95°. As collision energy is further increased to 6.4 eV in Figure 5, this product ion becomes forward scattered with a most probable scattering angle of 60°. The significant decrease in the scattering angle for NO_2^+ formation with increasing collision energy indicates that large impact parameter collisions begin to play a more important role as energy is increased.

These changes in the scattering pattern in the low collision energy range (Figures 3–5) can be qualitatively rationalized by the reactive line-of-centers (LC) model[34] assuming that the colliding species are structureless spheres which do not interact with each other until some critical separation is reached. The impulsive character of the excitation mechanism suggests that this model may account for gross scattering features of this mechanism. If the critical energy for dissociation is E_0, and the critical separation distance is d, the maximum value of the impact parameter at which this energy is reached, b_{max}, is related to collision energy, E_T, as follows:

$$b^2_{max} = d^2(1 - E_0/E_T) \quad (8)$$

It can be seen that this simplistic model predicts that b_{max} decreases as E_T decreases. Therefore, at low collision energies reaction is possible only for small impact parameter collisions that cause large angle scattering and only a rebound mechanism of the fragment ions can be observed at sufficiently low energies.

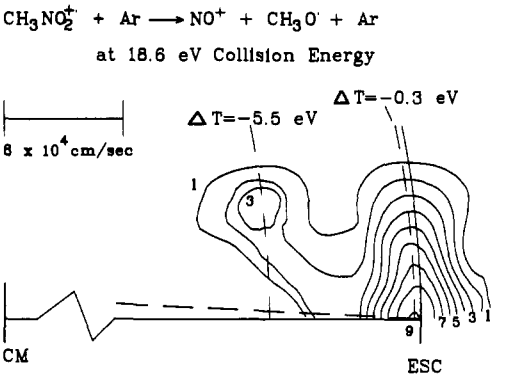

Figure 12. CM velocity contour map for the CID of nitromethane ion to NO^+ on collision with Ar at 18.6-eV collision energy. The circle marked $\Delta T = -5.5$ eV corresponds to transfer of 5.5-eV energy into internal excitation of the dissociating nitromethane ions. CM and ESC denote center-of-mass and elastic scattering circle, respectively, and the numbers represent relative intensities of each contour.

CM velocity contour maps for reaction 5 at 19.5-, 40-, and 119-eV collision energy are shown in Figures 6–8. These diagrams demonstrate that the most probable scattering angle decreases smoothly as collision energy increases but never approaches zero. Significant angular scattering of product ions occurs at all collision energies. This observation is similar to previous results for the CID of acetone and propane ions at medium and high collision energies,[27,28,33,35] indicating that impulsive collisions with extensive

(33) Herman, Z.; Futrell, J. H.; Friedrich, B. *Int. J. Mass Spectrom. Ion Processes* **1984**, *58*, 299.
(34) Smith, I. W. M. *Kinetics and Dynamics of Elementary Gas Reactions*; Butterworths: London, 1980.
(35) van der Zande, W. J.; de Bruijn, D. P.; Loss, J.; Kistemaker, P. G.; McLuckey, S. A. *Int. J. Mass Spectrom. Ion Processes* **1985**, *67*, 161.

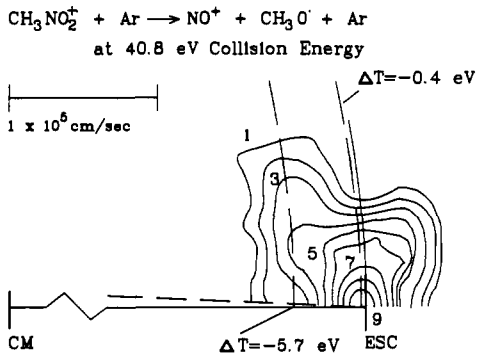

Figure 13. CM velocity contour map for the CID of nitromethane ion to NO^+ on collision with Ar at 40.8-eV collision energy. CM and ESC denote center-of-mass and elastic scattering circle, respectively, and the numbers represent relative intensities of each contour.

linear and angular momentum exchange dominate the CID reactions of these polyatomic ions. This qualitatively similar behavior for three molecular ions whose CID mechanisms are quite different demonstrates that scattering features become less dependent at higher collision energy on the nature of the ions and the excitation mechanisms involved.

Relative translational energy distributions shown in Figure 9 for reaction 5 at various energies were obtained by integrating over all scattering angles using eq 7. The most probable energy transfer for this process increases only slightly from 1.6 to 1.9 eV when collision energy is increased from 3 to 119 eV. This result is consistent with the interpretation that the dissociation rate for a direct bond dissociation process increases rapidly as the internal energy exceeds the critical energy of the process, and increases only slowly thereafter. The two unusual observations are that NO_2^+ was not detected with measurable intensity below 1.5-eV collision energy and that these energy transfers are all well above the threshold energy (1.0 eV) for the reaction. This point is especially striking if one considers that the reacting ions may contain substantial excess internal energy when they are formed by 70-eV electron ionization. This differs significantly from the analogous C–C bond cleavage in the propane molecular ion,[25,28,33] an archetypical example of a molecular ion whose decomposition is well described by the QET/RRKM theory, for which the most probable energy deposition is much closer to the threshold energy. On the basis of the apparent threshold and mean energy deposition above threshold, it is plausible that ground-state nitromethane ions are collisionally excited to low-lying electronically excited states (e.g., the second and third ionization bands in Figure 1) which are strongly coupled to the ground state and that rapid intramolecular relaxation preceeds dissociation. However, we do not observe any special features in the scattering contour maps that support this view.

Isomerization Process. Formation of NO^+. Since fragmentation of nitromethane ion to NO_2^+ requires 1 eV, and isomerization 0.64 eV, isomerization and subsequent dissociation to NO^+ compete very effectively with the formation of NO_2^+ at low collision energy. The dissociation of nitromethane ions into NO_2^+ and NO^+ follow two distinct pathways—NO_2^+ via direct C–N bond cleavage and NO^+ via isomerization to $CH_3ONO^{\cdot+}$. This accounts for the observation of a strong metastable ion[2,4,8b] for NO^+ while NO_2^+ is formed only by CID. It is also plausible that significant differences in the dynamics for these two reaction channels might be observable.

The formation of NO^+ from $CH_3NO_2^{\cdot+}$ involves the cleavage of C–N and N–O bonds and the formation of a new C–O bond. This can take place either as a two-step mechanism, isomerization to methyl nitrite ion followed by dissociation, or via a "tight" transition state (rearrangement) as the dissociation proceeds. Both mechanisms involve energy barriers not present in single bond dissociation. It has been shown by both metastable ion and CID studies that the nitromethane ion can isomerize to the energetically favored (more stable) methyl nitrite ion which later dissociates via simple O–N bond cleavage.[1,4] The barrier to isomerization has been estimated to be 0.64 eV, and ions interconverting to the methyl nitrite ion must have an excess energy of 1.27 eV.[7,8] Fragmentation of $CH_3ONO^{\cdot+}$ to NO^+ requires 0.45 eV, and all ions crossing the barrier must have sufficient internal energy for dissociation. These energy relationships have been summarized in Figure 2.

Figures 10 and 11 show velocity contour maps for NO^+ formation at collision energies of 1.5 and 3.0 eV, respectively. A remarkable feature of both diagrams is the observation of nearly symmetric forward- and backward-scattered peaks with scattering angles of 0° and >170°. Forward–backward symmetry is traditionally interpreted as evidence for formation of an orbiting complex between the ion and neutral that survives several rotational periods before fragmentation. However, in this case the kinetic energy is so much larger than the binding energy for the expected ion–neutral attractive potential between $CH_3NO_2^{\cdot+}$ and He that an alternative explanation must apply. We therefore suggest that NO^+ ions in the forward- and backward-scattered sectors are formed by two dynamically different mechanisms.

Further support for this conclusion is obtained by approximate calculations for the rotational frequency of the putative complex. The limiting value of the impact parameter for which the particles spiral into a circular orbit is given by[36]

$$b_0 = \left(\frac{4e^2\alpha}{\mu u_0^2}\right)^{1/4} \tag{9}$$

where e is the electronic charge, α is the electric polarizability of the neutral, μ is the reduced mass and u_0 is the relative velocity. For the nitromethane ion colliding with helium at 1.5-eV relative collision energy, b_0 is therefore equal to 0.8 Å. If we assume that the total relative energy is converted into the rotational motion, the rotational period for nitromethane–He complex is[37]

$$\tau_{rot} \cong 2\pi\left(\frac{\mu b_0^2}{2E}\right)^{1/2} \tag{10}$$

where E is the relative collision energy. From eq 10, we calculate a rotational period of 5.8×10^{-14} s, which is an order of magnitude shorter than typical rotational periods in a molecule. The collision time between nitromethane ion and He for 1.5-eV collision energy is 1.8×10^{-14} s for a total distance of 1.6 Å, which is much shorter than the rotational time of 5.8×10^{-14} s. We can therefore conclude that the apparent forward–backward symmetry observed for NO^+ from nitromethane ion at 1.5-eV collision energy is not a result of forming a long-lived complex in the collisional excitation step.

The appearance potential of NO^+ from $CH_3NO_2^{\cdot+}$ is 0.7 eV, while that of NO^+ from the methyl nitrite isomer is only 0.4 eV. As shown in Figures 10 and 11, these data and the relevant potential energy hypersurface are shown schematically in Figure 2. The forward-scattering mechanism, which requires only 0.1–0.2-eV conversion of translational-to-internal energy conversion involves a fraction of the nitromethane cations very near the barrier height that ergodically approach the transition-state configuration. Electron impact ionization of CH_3NO_2 produces a fraction of nitromethane molecular ions with a range of internal energy limited by the lowest energy barrier height to decomposition, about 0.64 eV in the case of the nitromethane cation. Consequently large impact parameter collisions by this population of highly vibrationally excited ions that can be described as highly excited ions approaching the methyl nitrite conformation result in decomposition into NO^+ following "soft collision" with very little momentum exchange. This mechanism is characterized by small energy transfer and a small scattering angle (maximizing at zero).

Close inspection of Figures 10 and 11 and the integration of the back-scattered peak over angles $\pi/2$ to π show that the second

(36) McDaniel, E. W. *Collision Phenomena in Ionized Gases*; John Wiley: New York, 1964.
(37) Berry, R. S.; Rice, S. A.; Ross, J. *Physical Chemistry*; John Wiley: New York, 1980.

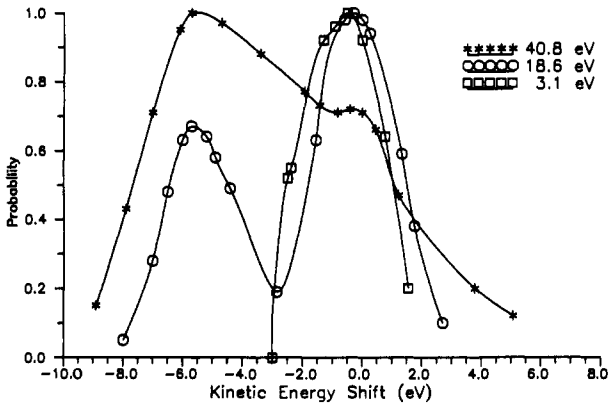

Figure 14. Relative translational energy distribution of NO^+ ions obtained from Figures 10–13 using eq 7.

NO^+ mechanism is more endothermic by about 0.3 eV. We suggest that the backward-scattered peak originates from the impulsive CID of a population of vibrationally excited $CH_3NO_2^{\bullet+}$ ions (occurring via small impact parameter collisions) that are located somewhat lower in the potential well and are activated by "hard collisions" that move them energetically to the top of the barrier and induce the nuclear motion required for rearrangement to the methyl nitrite structure. These NO^+ ions are likely the same population of precursor ions as those which form NO_2^+, which also exhibit backward scattering at 3.0-eV collision energy (see Figure 3). If these two mechanisms follow the same dynamics, low-energy deposition generates NO^+ while higher excitation leads to NO_2^+.

Once the methyl nitrite ion is formed with 0.8 eV more than the minimum energy for dissociation (see Figure 2), it proceeds diabatically along the potential surface to form NO^+. Leyh-Nihant and Lorquet have thoroughly discussed this particular example of unimolecular reactions following a nonadiabatic pathway.[20] The relative probability for retaining constant electronic configuration and dissociating to NO^+ on the diabatic surface was estimated to be 10^4 greater than that of following the adiabatic surface in a single passage through the critical region. This rationalizes many of the puzzling features about methyl nitrite cation decompositions. It also rationalizes the absence of CH_2OH^+ as a significant CID product and the prompt decomposition of $CH_3NO_2^{\bullet+}$ collisionally energized by the two low-energy mechanisms we have described.

Figures 12 and 13 display velocity contour diagrams for reaction 6 at 18.6- and 40.8-eV CM collision energies, respectively. No backward-scattered peak is observed at those energies, consistent with our earlier discussion suggesting that higher collision energies favor larger impact parameter CID. However, two distinct peaks in the forward-scattered region are still observed. At 18.6-eV CM collision energy, the two peaks are clearly separated, with one peak located near the relative velocity vector and the other at a scattering angle of about 8°. The two peaks are characterized by energy transfers of 0.3 and 5.5 eV at 0° and 8°, respectively, as shown in the relative translational energy distribution for this energy in Figure 14. Although the two peaks are no longer clearly resolved at 40.8 eV, the CID peak for the large energy transfer mechanism is now the predominant CID mechanism. We infer that this high-energy mechanism is dominant at collision energies above 40 eV. This readily accounts for the conclusion by Harrison and co-workers[11] that collisions deposit anomalously large amounts of energy in nitromethane cations.

We suggest that the small energy transfer, forward-scattered CID peak originates from nitromethane ions which have traversed the methyl nitrite cation isomerization path, the same mechanism discussed above. These internally excited methyl nitrite ions are excited above the dissociation limit via large impact parameter collisions with argon and dissociate into NO^+ and $CH_3O^{\bullet}$. The unexpectedly large energy transfer of about 5.5 and 5.7 eV in Figures 12 and 13 clearly arises from a different mechanism. We suggest that dissociation to NO^+ proceeds in parallel on two distinct potential energy surfaces at this energy and that the high energy transfer peak originates from ions retaining the nitromethane structure. Exciting nitromethane ions by adding 5.7-eV internal energy causes them to decompose faster than they can randomize energy among all internal degrees of freedom. This characteristic excitation mechanism is responsible for the discrete structure obtained in the scattering contour diagrams in Figures 12 and 13.

PEPICO experimental results provide useful information supporting this interpretation of this high energy loss CID mechanism. As shown in Table I and Figure 1, the sixth ionization band of nitromethane is located 5.7 eV above the ground state. The fact that our energy-transfer measurement matches the energy gap between the ground state and the sixth ionization band ($^2A_1$ state) of nitromethane ion[38] suggests that electronic excitation from the ground state is the operative activation mechanism. A relatively well separated and strong peak for the sixth band in the photoelectron spectrum (Figure 1) demonstrates that this transition has a favorable Franck–Condon factor. It is therefore highly probable that ions are excited to this state when sufficient energy is available to do so. If these ions randomize energy among all internal states, nitromethane ions would have a very broad distribution of energy in the ground state, resulting in a broad fragment ion peak distribution. This is not observed experimentally. PEPICO experiments have also shown that nitromethane ions excited to this energy state preferentially dissociate into NO^+; this appears as the second rise in NO^+ intensity in the breakdown graph in Figure 1. Indeed, it is the sharp rise in NO^+ formation at 5.7 eV above the ionization potential in the Figure 1 breakdown graph that is responsible for our being able to resolve this dynamics feature clearly in the contour diagrams. Our experimental results are also consistent with the Figure 1 breakdown graph result that much less NO_2^+ than NO^+ is observed when nitromethane ions are excited by 5.7 eV. Only a diffuse low-intensity tail of NO_2^+ is visible in that energy range in the contour diagrams shown in Figures 5 and 6.

The hypothesis that NO^+ may dissociate directly from the sixth electronic state of nitromethane is further supported by kinetic energy release distribution measurements.[3] At high internal energy range (5–6 eV), the mean kinetic energy release is significantly lower than that predicted by RRKM theory if internal energy is completely randomized in both electronic and vibrational modes. From these results, we can propose that the sixth electronic state of nitromethane ion is weakly coupled to the ground-state potential surface and energy randomization is slower than dissociation. The fact that the decrease in the abundance of NO_2^+ does not correlate with the increase in the abundance of NO^+ substantially rules out the possibility that NO^+ is produced from the secondary dissociation of NO_2^+, as suggested earlier by Ogden et al.[3]

It is interesting to note that a recent theoretical and experimental analysis of the CID of H_2^+ by He as a function of internal vibrational state preparation of the reactant ion and collision energy provides clear evidence that a significant fraction of the H^+ products are formed on the first excited-state potential energy surface.[39-41] Specifically, nearly all protons generated from CID of H_2^+ (v = 0, 1) at 3.1-eV collision energy result from electronically nonadiabatic transitions. A substantial fraction of H_2^+ (v = 4–6) also are formed via a nonadiabatic transition to the first excited-state hypersurface. This occurs when the system explores regions where the internuclear distances are comparable in this three-particle system. For v = 0 or 1, this requires hard collisions that stretch the H–H bond; for high vibrational states, glancing collisions suffice. Under these conditions, the separation between the ground- and excited-state hypersurfaces is sufficiently small

(38) Rabalais, J. W. *J. Chem. Phys.* **1972**, *57*, 960. In ref 16, we quoted it as the fifth ionization band on the basis of this reference. However, more recent work (ref 18) quotes this band as the sixth ionization band. Our interpretation (involving isolated electronic state(s)) does not change in any case.

(39) Govers, T. R.; Guyon, P. M. *Chem. Phys.* **1987**, *113*, 425.

(40) Gislason, E. A.; Guyon, P. M. *J. Chem. Phys.* **1987**, *86*, 677.

(41) Sizun, M.; Parlant, G.; Gislason, E. A. *J. Chem. Phys.* **1988**, *88*, 4294.

that nonadiabatic transitions become probable events even at low collision energy.[39,40]

Our study of acetone cation CID provides evidence for analogous behavior of a polyatomic ion at low collision energy. In this system, we identified an unexpectedly long-lived excited state that is scattered inelastically and dissociated in low-energy collisions.[17] We have measured its lifetime and the threshold energy[42] for inducing its nonadiabatic transition to the ground state, which then dissociates. We have also demonstrated the microscopic reversibility of the process as inelastic scattering in both bound-bound and bound-unbound transitions.[43] We suggested that a nonadiabatic curve crossing mechanism at small He-M^+ distances was responsible for this CID reaction at low collision energy and that higher excited states were excited in a similar mechanism at high collision energy. The nitromethane cation CID reactions reported here appear to be a second example of this kind of reaction dynamics for polyatomic ions. These results further demonstrate the hitherto unexpected importance of electronic excitation mechanism in the collisional activation/dissociation of polyatomic ions at moderate collision energies.

Conclusions

This investigation of nitromethane ion CID demonstrates that the formation of NO_2^+ and NO^+ proceeds via different reaction pathways. NO_2^+ ions are mostly formed from ions excited by an impulsive mechanism occurring via small impact parameter collisions and accompanied by large angular momentum exchange. NO^+ ions are produced from at least two quite different reaction channels. The lowest energy dissociation path generates NO^+ with modest energy deposition at zero scattering angle; we suggest this mechanism involves rearrangement of internally excited ions having structures approaching that of the transition state for forming methyl nitrite ions prior to the collisional activation step. The high-energy mechanism for generating NO^+ by deposition of 5.5-5.7 eV proceeds from an excited-state surface of the nitromethane ions.

We conclude that the CID of nitromethane ion to NO^+ and $CH_3O^\bullet$ is the second example we have found for remarkably efficient conversion of translational energy into electronic excitation in the low and medium collision energy ranges and inefficient randomization of internal energy. Like acetone, it is an example of a polyatomic ion exhibiting the "weak assumption" QET behavior[44] in which a bottleneck to energy randomization prevents intramolecular relaxation to the ground state prior to dissociation. Nitromethane ion is a rather special case in other ways that suggest it exhibits several bottlenecks at branch points for nuclear rearrangements leading to specific dissociation mechanisms which are a strong function of internal energy.

Acknowledgment. Support of this research by the National Science Foundation, Grant No. CHE-8312069, is gratefully acknowledged. We thank Professor Tomas Baer for a very useful discussion of nuances in the unimolecular decay of the methyl nitrite cation and for sharing his data prior to publication.

Registry No. $CH_3NO_2^+$, 74868-54-5; CH_3ONO^+, 85232-65-1.

(42) Fenistein, S.; Futrell, J.; Heninger, M.; Marx, R.; Mauclaire, G.; Yang, Y. *Chem. Phys. Lett.* **1991**, *179*, 125.
(43) Qian, K.; Shukla, A.; Futrell, J. *Chem. Phys. Lett.* **1990**, *175*, 51.
(44) Lorquet, J. C. *Org. Mass Spectrom.* **1981**, *16*, 469.
(45) Kandel, R. J. *J. Chem. Phys.* **1955**, *23*, 84.
(46) Lias, S. G.; Bartmess, J. E.; Liebman, J. F.; Holmes, J. L.; Levin, R. D.; Mallard, W. G. *J. Phys. Chem. Ref. Data, Suppl.* **1988**, *17*.

Ab Initio SCF Calculations on Low-Energy Conformers of *N*-Acetyl-*N'*-methylalaninamide and *N*-Acetyl-*N'*-methylglycinamide

Hans-Joachim Böhm* and Stefan Brode

Contribution from BASF AG, Central Research and Informatics, 6700 Ludwigshafen, Germany.
Received March 27, 1990

Abstract: Results from ab initio SCF calculations with a double-ζ plus polarization (DZP) basis set on five low-energy conformations of *N*-acetyl-*N'*-methylalaninamide ("dialanine") and three conformations of *N*-acetyl-*N'*-methylglycinamide ("diglycine") are reported. In addition, data from calculations with a triple-ζ plus polarization (TZP) basis set on two conformations of diglycine are given. The results are used to assess the quality of current force fields aimed at peptides and proteins. The present ab initio data point to some important deficiencies of current protein force fields with respect to relative energies of dipeptide conformers.

1. Introduction

Accurate force fields are one of the most important tools in molecular modeling. Especially force fields for proteins and peptides are heavily needed in biochemical and drug design applications. Thus, several force fields such as AMBER,[1] ECEPP,[2,3] CVFF,[4,5] or CHARMM[6] have been proposed and are now widely used in force field calculations. However, the validation of a force field by comparing calculated energies and geometries with experimental data or high-quality quantum chemical ab initio calculations is difficult for several reasons.

Experimental structural information on peptides and proteins is only available for the condensed phase. Such a system is

(1) Weiner, S. J.; Kollman, P. A.; Case, D. A.; Singh, U. C.; Ghio, C.; Alagona, G.; Profeta, S.; Weiner, P. *J. Am. Chem. Soc.* **1984**, *106*, 765.
(2) Momany, F. A.; McGuire, R. F.; Burgess, A. W.; Scheraga, H. A. *J. Phys. Chem.* **1975**, *79*, 2361.
(3) Zimmerman, S. S.; Pottle, M. S.; Nemethy, G.; Scheraga, H. A. *Macromolecules* **1977**, *10*, 1.
(4) Stern, P. S.; Chorev, M.; Goodman, M.; Hagler, A. T. *Biopolymers* **1983**, *22*, 1885.
(5) Dauber-Osguthorpe, P.; Roberts, V. A.; Osguthorpe, D. J.; Wolff, J.; Genest, M.; Hagler, A. T. *Proteins* **1988**, *4*, 31.
(6) Brooks, B. R.; Bruccoleri, R. E.; Olafson, B. D.; States, D. J.; Swaminathan, S.; Karplus, M. *J. Comput. Chem.* **1983**, *4*, 187.
(7) Pettitt, B. M.; Karplus, M. *Chem. Phys. Lett.* **1985**, *121*, 194.

0002-7863/91/1513-7129$02.50/0